Geol. Mag. **154** (*6*), *2017, pp. 1269–1284.* © *Cambridge University Press 2017*
doi:10.1017/S001675681700053X

Chambered structures from the Ediacaran Dengying Formation, Yunnan, China: comparison with the Cryogenian analogues and their microbial interpretation

CUI LUO*†, BING PAN‡§ & JOACHIM REITNER¶

*CAS Key Laboratory of Economic Stratigraphy and Palaeogeography, Nanjing Institute of Geology and Palaeontology, 39 East Beijing Road, 210008 Nanjing, China
‡State Key Laboratory of Palaeobiology and Stratigraphy, Nanjing Institute of Geology and Palaeontology, Chinese Academy of Sciences, 39 East Beijing Road, 210008 Nanjing, China
§University of Science and Technology of China, 230026 Hefei, China
¶Department of Geobiology, Centre of Geosciences of the University of Göttingen, Goldschmidtstraße 3, 37077 Göttingen, Germany

(*Received* 29 November 2016; *accepted* 12 May 2017; *first published online* 29 August 2017)

Abstract – Enigmatic chambered structures have been reported forming reef frames in Cryogenian interglacial carbonates, prior to the commonly acknowledged microbial-metazoan reefs at the terminal Ediacaran, and interpreted as fossils of possible sponge-grade organisms. A better constraint on the affinity of these structures is partly hindered by few analogues in other time periods. This study describes similar structures from peritidal dolostones of the Ediacaran Denying Formation from Yunnan, China. Samples were investigated using optical microscopy and three-dimensional (3-D) reconstruction based on grinding tomography. The Dengying chambered structures are comparable with Cryogenian structures in basic construction, but are not frame building, and show variations in overall shape and inhabiting facies. Two-dimensional (2-D) cross-sections show that thin, homogeneous micritic laminae are the basic building blocks of the chamber walls. Thick walls represent parallel accretion of these laminae, and thin walls developed from the angular growth of a single lamina or merging of multiple laminae. In 3-D space, the laminae primarily correspond to continuous surfaces which sometimes contain sub-circular holes, while a few represent filamentous elements connected to the surfaces. The morphological features and growth pattern of the Dengying chambered structures indicate that they are likely to be calcified microbial constructions rather than skeletal remains of basic metazoans. However, aside from the Cryogenian and Dengying examples, comparable chambered constructions with laminae-based architecture are yet unknown from other fossil or extant microbialites. Further work investigating related structures is needed to determine the microbial consortia and controlling environmental factors that produced these chambered structures.

Keywords: Dengying Formation, chambered structures, microbialites, Ediacaran, sponges, carbonates.

1. Introduction

A series of environmental and evolutionary changes at the Neoproterozoic–Cambrian transition fundamentally shaped the Phanerozoic biosphere (Lenton *et al.* 2014; Erwin, 2015). One of these dramatic changes was the gradual substitution of metazoan-dwelled and -constructed reefs for microbial bioconstructions in carbonate environments. Before the advent of archaeocyathan-microbial reefs in early Cambrian time, the earliest putative metazoans with calcified skeletons, such as *Cloudina* and *Namacalathus*, were dwellers of complex microbialite systems (e.g. Grotzinger, Watters & Knoll, 2000; Grotzinger, Adams & Schröder, 2005). Recent studies suggested that they may have constructed biostromes, small mounds and columnar build-ups, at ~548 Ma in Namibia (Penny *et al.* 2014; Wood & Curtis, 2015). In addition to these putative metazoan fossils, some macroscopic chambered structures have been found forming reef frames in the Cryogenian carbonates in South Australia (Giddings, Wallace & Woon, 2009; Wallace *et al.* 2014, 2015), and distributed (but not evidently reef-forming) in the coeval strata in northern Namibia (Wallace *et al.* 2014). Although interpreted as possible 'proto-sponges, sponge-grade organisms, or complex microbial precursors to sponge-grade organisms' (Wallace *et al.* 2014), the affinity of these structures is still enigmatic, partly owing to the lack of closely comparable structures from other time periods.

This paper describes analogous chambered structures from the upper Ediacaran Dengying Formation, Yunnan Province, China. This is the first report of this

†Author for correspondence: cluo@nigpas.ac.cn

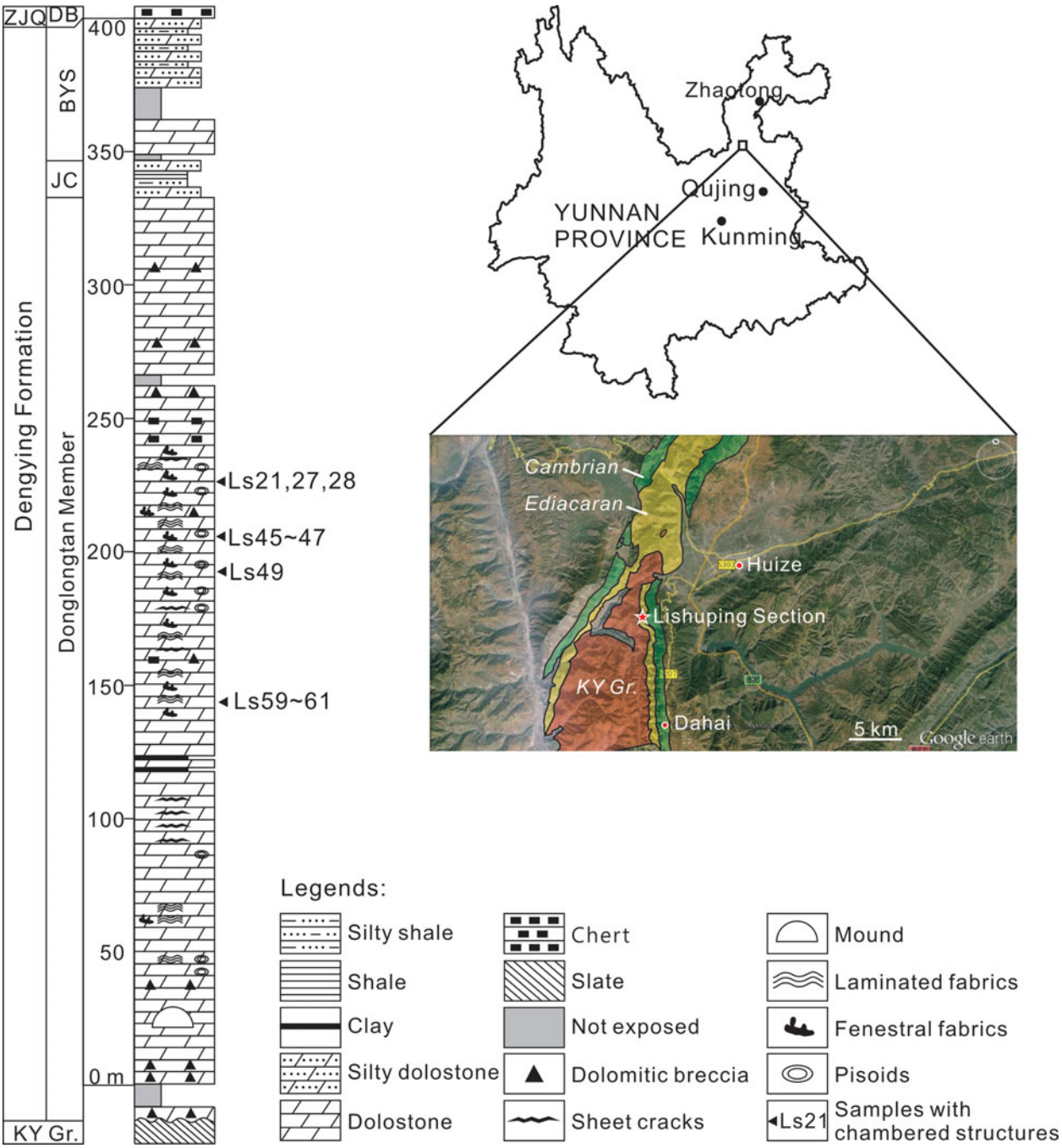

Figure 1. (Colour online) Location and stratigraphic log of the Lishuping Section. Abbreviations (in alphabetic order): BYS – Baiyanshao Member; DB – Daibu Member; JC – Jiucheng Member; ZJQ – Zhujiaqing Formation; KY Gr. – Kunyang Group.

type of structures outside of the Cryogenian, and the new materials provide further clues to decipher the provenance of these enigmatic structures.

2. Materials and methods

The studied materials were collected from an outcrop located ~10 km southwest of the centre of Huize County, adjacent to Lishuping Village, Yunnan Province, SW China (Fig. 1). In this region, Ediacaran deposits unconformably overlie the Kunyang Group, which was metamorphosed during the Jinning Movement at the Mesoproterozoic–Neoproterozoic transition. The hiatus corresponds to a period when the Huize region was a NNW–SSE-stretching hill and then an island, and not subject to deposition (Yunnan Bureau of Geology and Mineral Resources, 1995). In the investigated outcrop, the upper Ediacaran Dengying Formation directly overlies the Kunyang Group and conformably underlies the Daibu Member of the Zhujiaqing Formation (Fig. 1).

Exact chronological data are lacking for the investigated outcrop, but the age of the strata can be estimated through correlative rock units. A 551 Ma U–Pb zircon age, measured from the volcanic ash bed below the Dengying Formation in the Yangtze Gorges, is

https://doi.org/10.1017/S001675681700053X Published online by Cambridge University Press

broadly adopted as the lower chronological constraint for the Dengying Formation (Condon *et al.* 2005; Zhu, Zhang & Yang, 2007). Meanwhile, the most recent biostratigraphic studies of acanthomorphic acritarchs and small shelly fossils confirmed that the Daibu Member represents the lowermost Cambrian (Ahn, 2014; Yang *et al.* 2016). Therefore, the age of the investigated Dengying Formation is estimated as 551–541 Ma.

The Dengying Formation is subdivided into three members, namely the Donglongtan, Jiucheng and Baiyanshao members in ascending order (Fig. 1). The Donglongtan Member is a sequence of peritidal dolostones enriched with microbial deposits. With a hiatus at the base, the exposed part of this member is more than 300 m thick. The ancient water depth and terrestrial input increased during the deposition of the Jiucheng Member, resulting in a sequence of interbedded grey calcareous siltstone, greenish-grey shale and purplish silty shale, ~15 m thick. The Baiyanshao Member, ~53 m thick, consists of thick-bedded microcrystalline dolostones in the lower part, while fine siliciclastic components increase again in the upper part of this member.

Chambered structures were found in the Donglongtan Member only. Seventy-two rock samples were collected from this member and processed into 120 7.5×5.0 cm thin-sections. Polished slabs and thin-sections were observed using a Nikon SMZ18 and a Nikon ECLIPSE LV100NPOL microscope at the Nanjing Institute of Geology and Palaeontology, Chinese Academy of Sciences. A subset of thin-sections was further studied using a CL8200 Mk5-2 cathodoluminescence (CL) microscope at the Chinese University of Geosciences (Wuhan).

In order to investigate the three-dimensional (3-D) architecture of the chambered structures, a region of sample Ls45a was cut into a $3.6 \times 3.4 \times 0.5$ cm slab and ground stepwise using a Hillquist thin-section machine. Fifty planes were taken from this slab with a distance of 21.5 ± 3.4 μm between adjacent planes. The distances were controlled using a Mitutoyo micrometer. Each plane was manually polished using 3.5 μm silicon carbide, wetted and then scanned using an EPSON Scan L455 scanner with a resolution of 1200 dpi. The obtained images were initially aligned to each other using Adobe Photoshop CS3 Extended 10.0 and then built into a TIFF stack using ImageJ 1.49v. Using the software combination, the region of interest was cropped from the TIFF stack, and the contents of cement and host rock were removed from each plane, leaving only the chamber walls for 3-D reconstruction (Fig. 3a, c; 'chamber walls' cf. Section 3.b). Finally, the processed TIFF stack was adjusted to 8-bit greyscale mode and imported into Voreen 4.4 (http://voreen.uni-muenster.de) to visualize the 3-D architecture.

In addition to Ls45a, a part of sample Ls47 was also consecutively ground, polished and scanned. Because of the chamber system complexity and low contrast between the chamber walls and cement in this sample, these data were not further processed to create a 3-D model. However, this series of images also reveals the general growth habit of the chambers (Fig. 3e–g).

All studied samples and thin-sections are archived at the Nanjing Institute of Geology and Palaeontology, Chinese Academy of Sciences.

3. Results

3.a. Microfacies of the Donglongtan Member

The exposed part of the Donglongtan Member exhibits evaporitic peritidal facies. Autochthonous microcrystalline dolomitic deposits with fenestral and laminated fabrics are dominant from the base of the measured outcrop, at 0 m, to ~230 m. Microbial bindstone, grainstone and packstone with sand-sized intraclasts occur sporadically as layers or lenses (e.g. Fig. 2a), reflecting the temporary influence of agitated water. Pisoids showing inversely graded bedding, an irregular shape and bridged coats are also common (Fig. 2c). Euhedral pseudomorphs of gypsum were observed at several levels as indicators of an evaporitic environment (Fig. 2a). In addition, some keg-barrel-shaped pseudomorphs were probably left by anhydrite crystals (Fig. 2b, cf. Warren, 2006, p. 39).

The upper part of the exposed Donglongtan Member, from ~230 m to ~330 m of the measured outcrop, is dominated by microbial bindstone with silt- to sand-sized intraclasts. Many clasts exhibit a dark microcrystalline envelope and bright sparitic centre (Fig. 2e, f). Similar clasts were once interpreted as remnants of the calcimicrobe *Renalcis* (e.g. Zhu & Luo, 1992). However, compared with *Renalcis* (cf. Pratt, 1984; Riding & Voronov, 1985; Riding, 1991), these clasts have much thinner microcrystalline 'walls' and more irregular shapes. Some are elongated or even rectangular in thin-section, indicating that they are rather cortoids than calcimicrobes. Nonetheless, the elements with microcrystalline rims and sparitic centres at the level of 228 m may have a different origin from the intraclasts; the elongated or even filamentous forms can occur together with rounded forms within a 1×1 mm area, and the former can be contorted around or truncated by some early lithified cavities (Fig. 2d). Redeposition of indurated clasts rarely results in such a state of organization.

3.b. Description of the Dengying chambered structures

Chambered structures were found at several levels where fenestral and laminated fabrics are developed (Fig. 1). Based on morphological features and the host rock fabric, these structures are here classified into two types, DYC-1 (Denying chambered structure type-1) and DYC-2 (Denying chambered structure type-2), and described separately.

DYC-1 developed within microcrystalline dolostone with fenestral fabrics. In hand specimen, it appears as

https://doi.org/10.1017/S001675681700053X Published online by Cambridge University Press

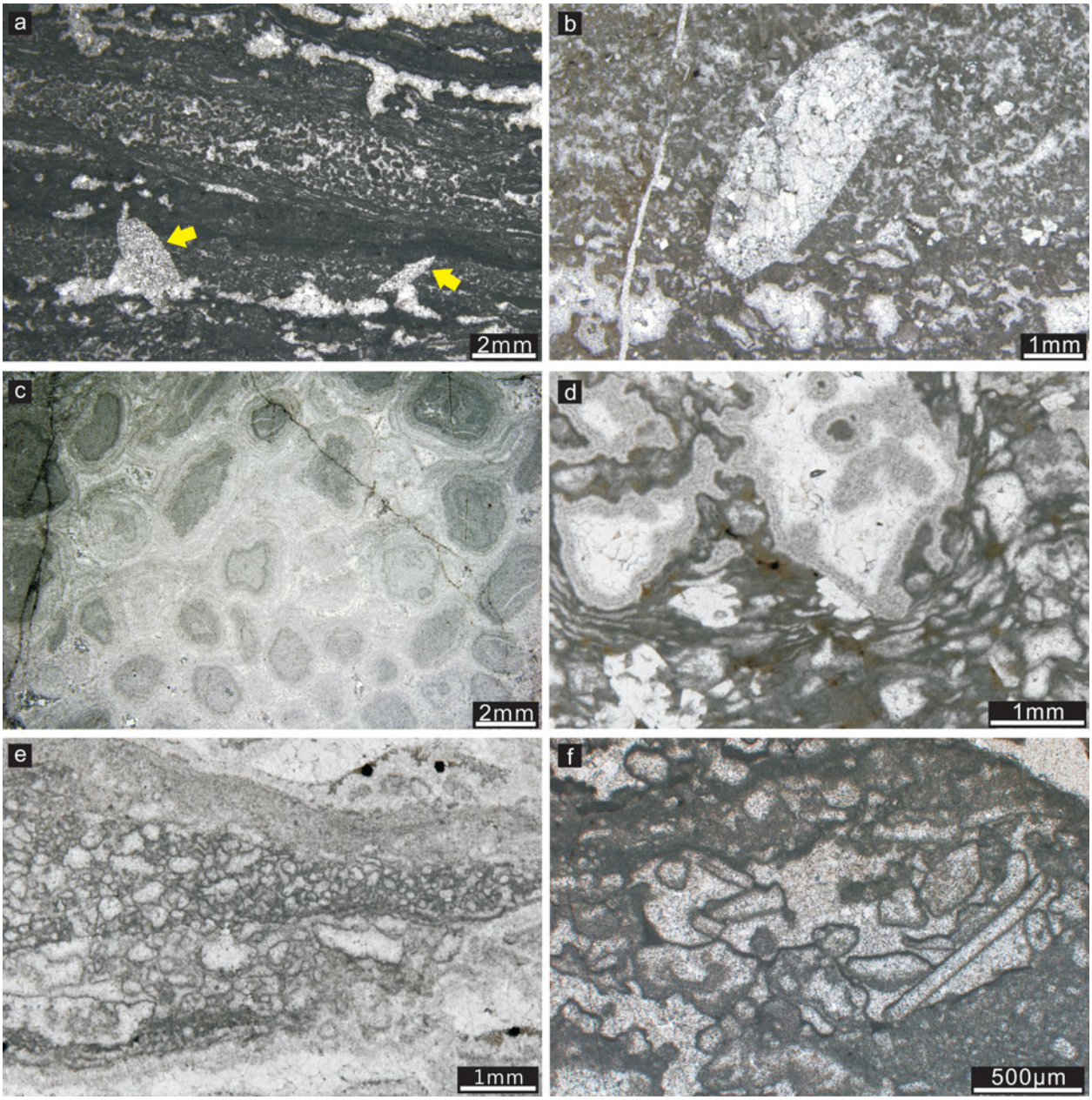

Figure 2. (Colour online) Sedimentary structures in the Donglongtan Member. (a) Lenticular deposits of peloidal grainstone intercalated in fenestral fabric. Two gypsum pseudomorphs are indicated with arrows. (b) A keg-barrel-like pseudomorph, probably left by an anhydrite crystal. (c) Pisoids. (d–f) Structures composed of elements which contain thin, dark micritic envelopes surrounding bright sparitic centres. Among them, (e) and (f) are obvious allochthonous deposits of cortoids bound by microbial laminae, while (d) is likely autochthonous microbial deposits. All photos are oriented upwards. Sample numbers: (a) Ls36; (b) Ls23; (c) Ls35c; (d) Ls22; (e) Ls03; (f) Ls14.

millimetric to centimetric, spar-cemented sheet cracks or large fenestral cavities (Fig. 3a, c, d). While observed under the microscope, they are generally composed of a thick wall, which separates the cavity from the host rock, and thin walls, which divide the cavity into polygonal subordinate spaces (Figs 4a, 5a, b). However, in some places, the thick wall is absent and the cavity boundary merely defined by a thin wall (e.g. Fig. 4c, indicated with the solid arrow in Fig. 5d). Here we temporarily and intuitively adopt the word 'wall' to describe these structures because they separate spaces when observed in thin-section, consecutively ground planes and 3-D images (details in the description that follows). The true nature of these structures will be further discussed in Sections 4.b and 4.c.

The thick walls exhibit variable thicknesses up to hundreds of micrometres and a laminated inner structure in well-preserved samples (e.g. Fig. 5d, e). In other samples, the lamination can be vague (e.g. Fig. 4d) or even indiscernible (e.g. Fig. 4b). The outer rim of the thick wall, which is in direct contact with the host rock, shows an irregular outline (e.g. Fig. 4a, b, d, e). In contrast, the inner rim deviates from the shape of the outer rim and tends to form a rather smooth curve (e.g. Figs 4a, b, d, e, 5a–d). In some samples, the innermost lamina of the thick wall overgrows the deformation of

https://doi.org/10.1017/S001675681700053X Published online by Cambridge University Press

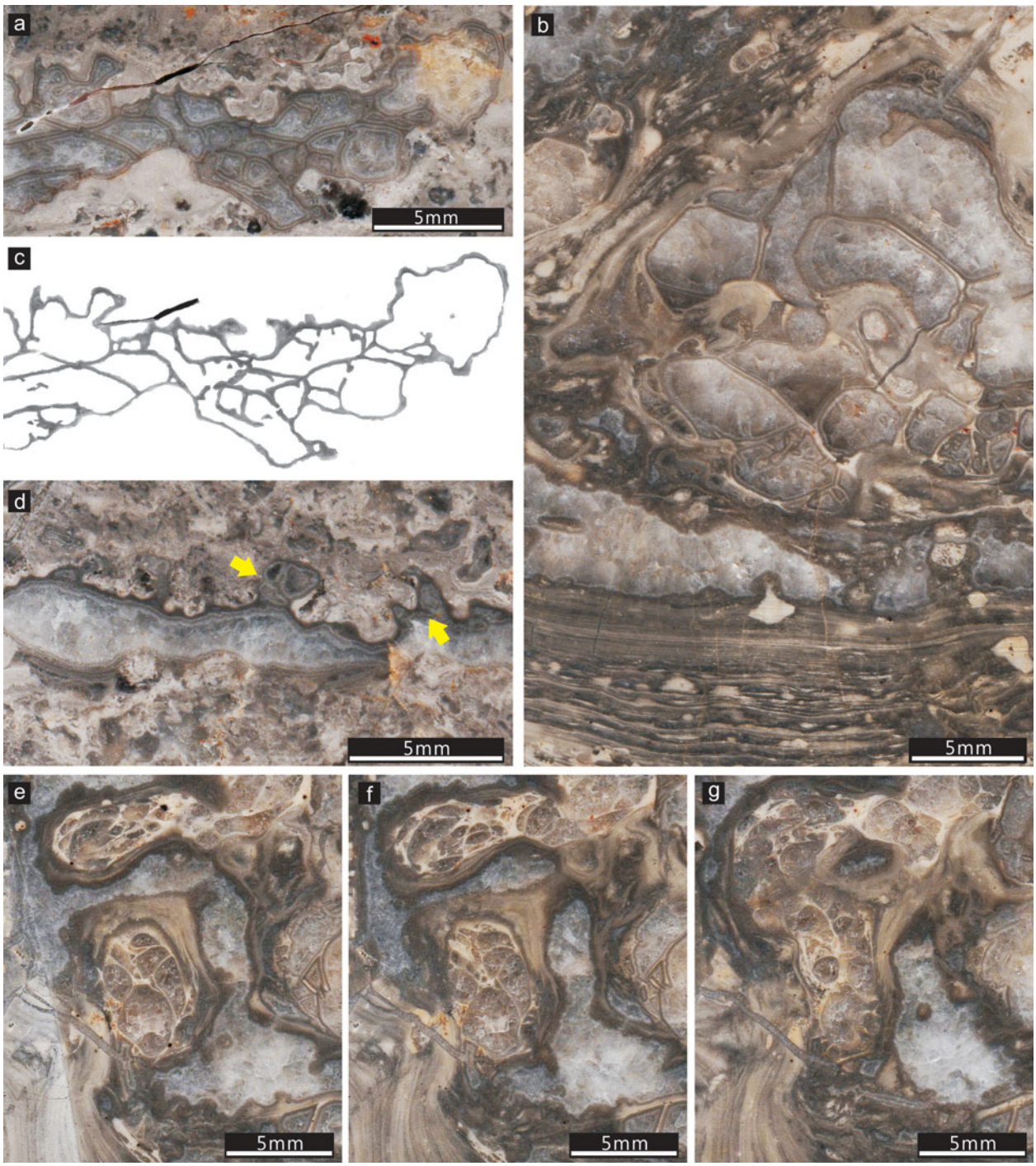

Figure 3. (Colour online) Chambered structures in polished slabs. (a, c, d) Dengying chambered structure type-1 (DYC-1), sample Ls45a. (a) The first plane of the consecutively ground DYC-1 sample Ls45a. (c) The processed image of the first plane, in which cement and host fabrics were removed, only the chamber walls remaining. The image was adjusted to an 8-bit greyscale mode before importing into Voreen. (d) A chambered structure whose thin walls are not well developed, but are visible in the arrowed places. A thin-section photo of this kind of chamber is shown in Figure 7a. (b, e–g) Dengying chambered structure type-2 (DYC-2), sample Ls47. (e–g) Part of the consecutively ground planes of sample Ls47, showing the spar-cemented growth cavity between two bulbous chambers. All photos are oriented upwards.

earlier laminae (Fig. 5c, g). At the contact with the thick walls, the host rock often exhibits a grumelous texture (Figs 4b, 5c, d).

Gaps cemented by microspars are sometimes present between the thick wall and host rock. In some, the gap margin is irregular and defined by the shape of neomorphic crystals (indicated with solid arrows in Fig. 4b, d, e), indicating that these structures were probably formed owing to neomorphism or overprinted by this process. This phenomenon is also observable in some thin walls (Fig. 8g). In the others, the gap margin is smooth (indicated with hollow arrows in Figs 4b, d, e, 5d), indicating that the cement crystals grew in pre-existing spaces. These spaces were likely

https://doi.org/10.1017/S001675681700053X Published online by Cambridge University Press

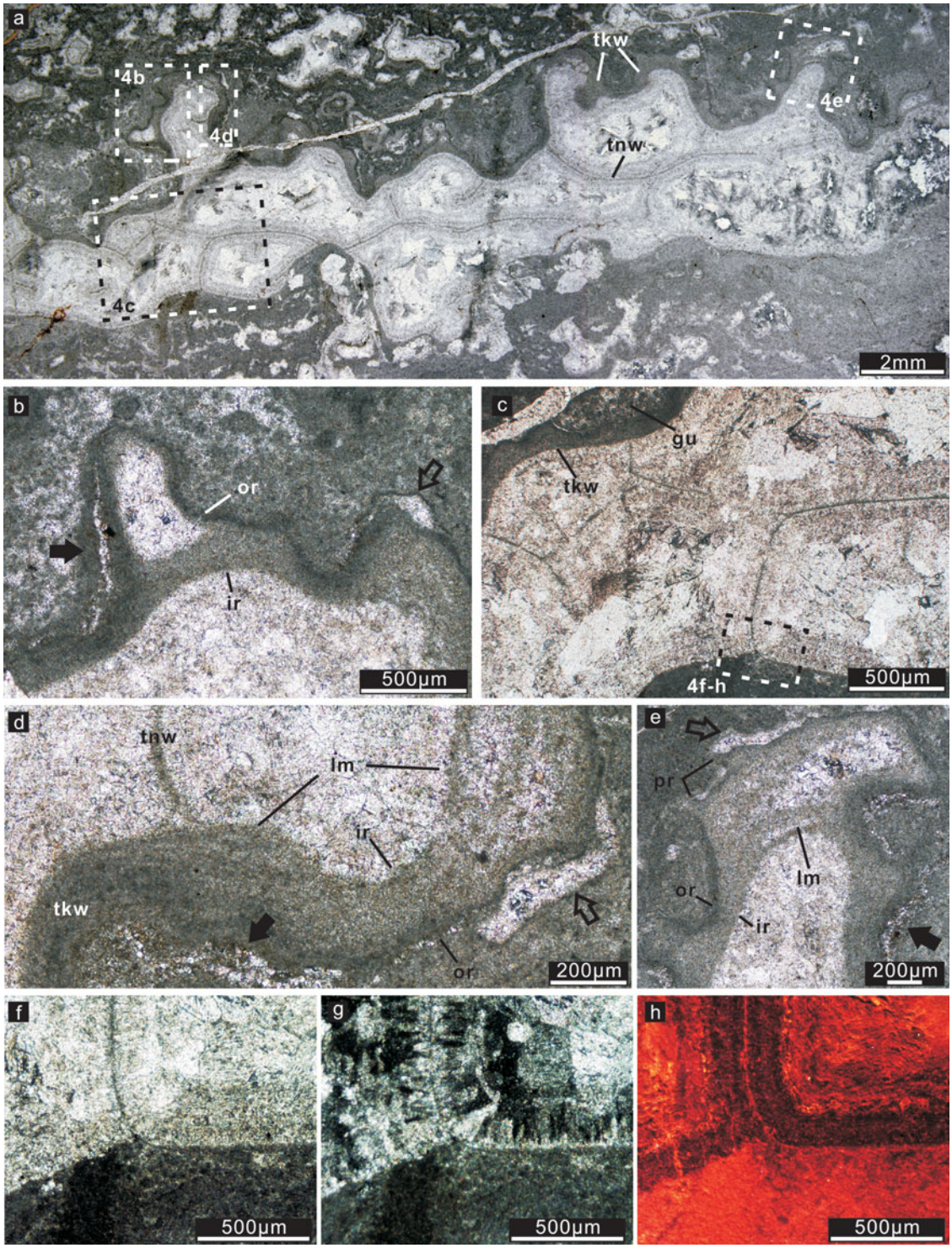

Figure 4. (Colour online) (a) Overview of a sheet-crack-like DYC-1 sample in thin-section, oriented upwards. The areas in dashed rectangles are enlarged in (b–e) with rotation of different angles. (b) The grumelous fabric of the host rock, thick wall and gaps between them. The two types of gaps are indicated with solid and hollow arrows (see Section 3.b in the main text for details). (c) Showing where the thick wall is present at the chamber ceiling and absent at the bottom. The area in the rectangle is enlarged in (f–h). (d) Showing part of the thick wall where the laminated inner structure is vague but discernible. A thin wall is connected to the inner rim of the thick wall with a cuspate structure. The two types of gaps between the thick wall and host rock are indicated with solid and hollow arrows, respectively. (e) Enlarged view of the small protrusions on the upper surface of the chambered structures. (f–h) Enlarged view of the area in the rectangle in (c) under plane-polarized light (f), crossed polarized light (g) and CL (h). The thin wall in this part is in direct contact with the grumelous fabric in the host rock, and is overgrown by bladed, isopachous cement that exhibits dull CL. Abbreviations (in alphabetic order): ir – inner rim; lm – laminated structure; or – outer rim; pr – protrusion; tkw – thick wall; tnw – thin wall. Sample number: Ls45a.

https://doi.org/10.1017/S001675681700053X Published online by Cambridge University Press

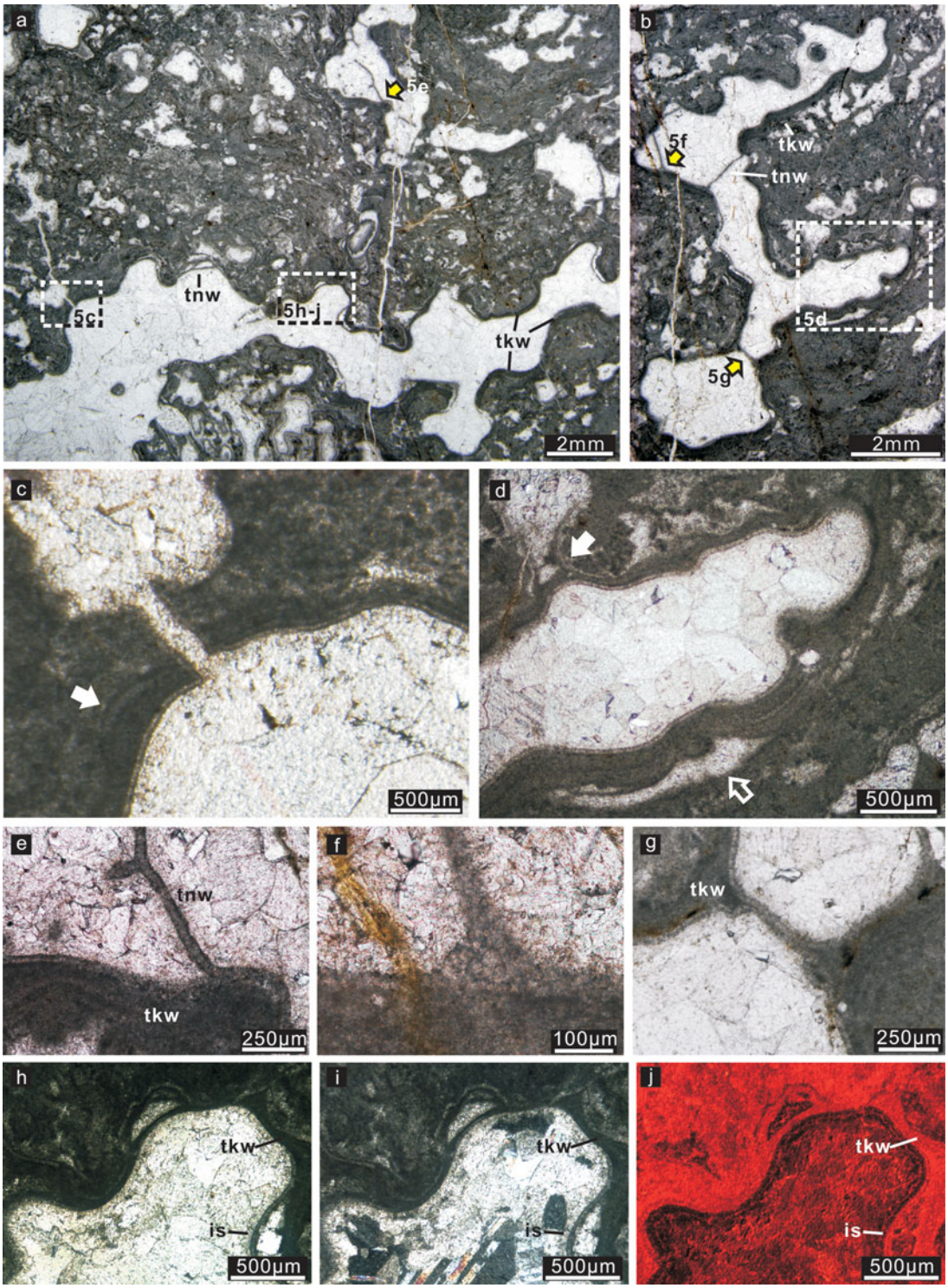

Figure 5. (Colour online) (a, b) Overview of fenestrae-filling DYC-1 in thin-section. Arrows and dashed rectangles indicate places which are enlarged in (c–j). (c) The innermost lamina of the thick wall overgrows a fissure in earlier laminae. The arrow indicates where a lamina in the thick wall is separated from other laminae. (d) A part of (b), exhibits well-preserved lamination in the thick wall. A gap between the thick wall and host rock is indicated with a hollow arrow. The solid arrow indicates where a lamina diverges from the thick wall and directly contacts the host rock. (e) The innermost lamina of the thick wall diverges from other laminae to form a thin wall. (f) A thin wall is connected to the innermost laminae of the thick wall with a cuspate tubercle. (g) The innermost lamina of the thick wall overgrows the tubercles formed by earlier laminae. (h–j) The same area under plane-polarized light (h), crossed polarized light (i) and CL (j), where the chamber wall is immediately overgrown with a thin, isopachous cement, which exhibits dull CL. Abbreviations: is – isopachous cements; for others see the caption of Figure 4. All photos are oriented upwards. Sample number: Ls45b.

https://doi.org/10.1017/S001675681700053X Published online by Cambridge University Press

formed during the growth or decay of the chambered structures.

Different from the thick walls, most thin walls retain a homogeneous inner structure and uniform thickness (Figs 4, 5). However, this thickness is variable among different specimens, from 20 μm to 100 μm. Thin walls are perpendicularly or obliquely connected to the thick wall with direct contact or cuspate tubercles (Figs 4c, d, 5f). Sometimes, the innermost lamina of the thick wall diverges from other laminae to form a thin wall (Fig. 5e).

According to the 3-D reconstruction of Ls45a, the thin walls are primarily smooth, uniform and continuous surfaces (Fig. 6 and Figs S1, S2 in the online Supplementary Material available at http://journals.cambridge.org/geo). Some of these surfaces bear subcircular holes (Fig. 6b–c, e), and are connected to short filamentous elements (Fig. 6d, e). The longitudinal cross-section of a filament may be indistinguishable from that of a surface when viewed in polished slabs.

Both thick and thin walls are now composed of microcrystalline dolomite, which emits red CL similar to the microcrystalline dolomite in the host rock (Figs 4f–h, 5h–j). These walls are immediately overgrown by bladed, isopachous cement, which exhibits dull CL. The remaining chamber spaces are filled with blocky dolomite spars.

In some DYC-1 samples, thin walls do not appear to be well developed or preserved compared with the archetype described above (Figs 3d, 7a, b). In one sample, multi-laminated structures resembling thick walls, without growth along the cavity wall, appear to have disassembled into several thin-wall-like laminae (Figs 7a, c, d). In another example, structures appearing like partially destroyed and strongly crinkled thin walls are preserved (Fig. 7b).

DYC-2 is characterized by millimetric to centimetric, bulbous or lenticular structures associated with laminated fabrics. These structures can encrust on (e.g. Figs 3b, e–g, 8a) or be intercalated in (e.g. Fig. 8b, c) microbial laminae. The subdivided chamber spaces are polygonal or lobate in form.

DYC-2 does not have a prominent thick wall like DYC-1. However, the laminae immediately surrounding the chambers are darker and more continuous than the others in the laminated fabrics (Fig. 8a, d, g, h).

The thin walls of DYC-2 are homogeneous in inner structure, but are not always regular in thickness (Figs 3b, c, 8a); although most maintain a thickness of 40–60 μm, a thickness of several hundreds of micrometres is found in a few places. Similar to that of DYC-1, the thin walls of DYC-2 can be connected to the surrounding dark laminae with direct contact or cuspate tubercles (Fig. 8c), or formed by a lamina diverging from others (arrows in Fig. 8a, d). In addition, some bundles of laminae converge to form a thin wall in DYC-2 (Fig. 8d–f). The consecutively ground planes of sample Ls47 demonstrate that most walls observed in 2-D cross-sections are continuous surfaces in 3-D space (Fig. 3e–g).

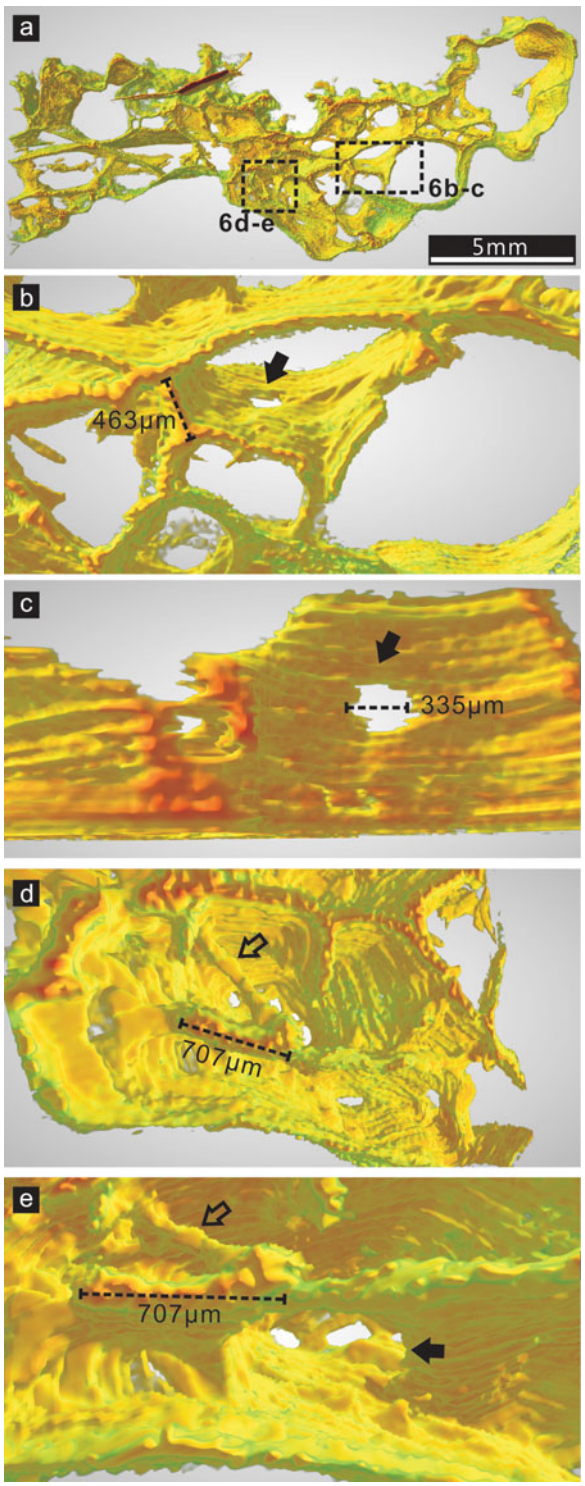

Figure 6. (Colour online) Three-dimensional (3-D) architecture of part of the DYC-1 sample Ls45a. A ground plane of this sample is shown in Figure 3a. The colours in the 3-D image correspond to the darkness of the original material in 8-bit greyscale mode: red and green represent the darkest and lightest parts, respectively; orange and yellow represent the moderate darkness between the two ends. (a) Overview of the 3-D model. The areas in rectangles are enlarged in (b–e). (b) A hole in the continuous surface of the thin wall, indicated with a solid arrow. (c) A closer view of the hole in (b). The thin walls above are clipped to better illustrate the hole. (d) A filament (hollow arrow) is connected with thin walls. (e) A rotated view of the structures in (d). The solid arrow indicates a hole in the surface.

https://doi.org/10.1017/S001675681700053X Published online by Cambridge University Press

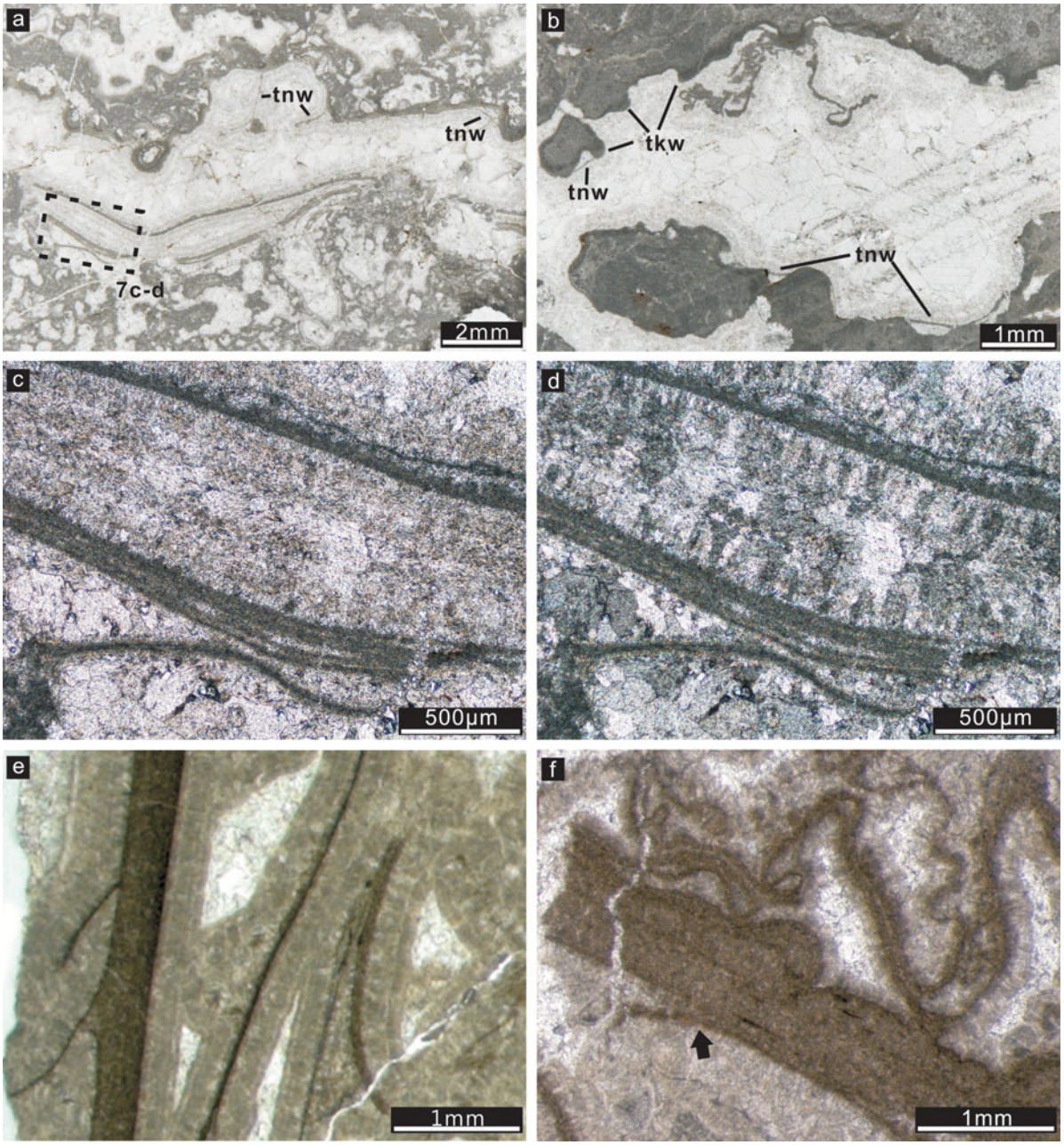

Figure 7. (Colour online) (a, b) DYC-1 samples in which thin walls are not well developed. The area in the dashed rectangle in (a) is enlarged in (c, d). The intensive contortion of the walls in the upper part of (b) possibly represents the ductile deformation of partially destroyed thin walls. A polished slab of this kind of DYC-1 is shown in Figure 3d. (c, d) Disintegration and contortion of the thick-wall-like multi-laminated structure, in plane and crossed polarized light, respectively. (e, f) Fragmented chamber walls from the Cryogenian Rasthof Formation, Namibia. (e) A thin wall is connected with the thick wall with a cuspate tubercle. (f) An individual lamina diverges from the multi-laminated thick wall (arrow), and some other laminae exhibit the same intensive contortion as shown in (b). The Namibian samples are now archived at the University of Göttingen, Germany. Abbreviations: see caption for Figure 4. Photos in (a–d) are oriented upwards. Sample numbers: (a–d), Ls45; (e, f) AAP 01 17.

The walls of DYC-2 are also immediately overgrown by bladed, isopachous cement, and the remaining chamber spaces are filled with blocky cement (Fig. 8e–h).

4. Discussion

4.a. Comparison with Cryogenian chambered structures

The Cryogenian chambered structures found in Australia and Namibia 'consist of multiple macroscopic and microscopic cavities…with walls consisting of micritic carbonate' (Wallace *et al.* 2014, p113); the walls are either thin and homogeneous, or thick and laminated. The DYC-1 and -2 described above are both consistent with these structures in basic construction: (1) all the Ediacaran and Cryogenian chambered structures are embedded in microbially induced fabrics; (2) they have multi-laminated thick walls and homogeneous thin walls; and (3) their chamber sizes, wall thicknesses and cement generations are comparable. A detailed comparison between the Cryogenian and

https://doi.org/10.1017/S001675681700053X Published online by Cambridge University Press

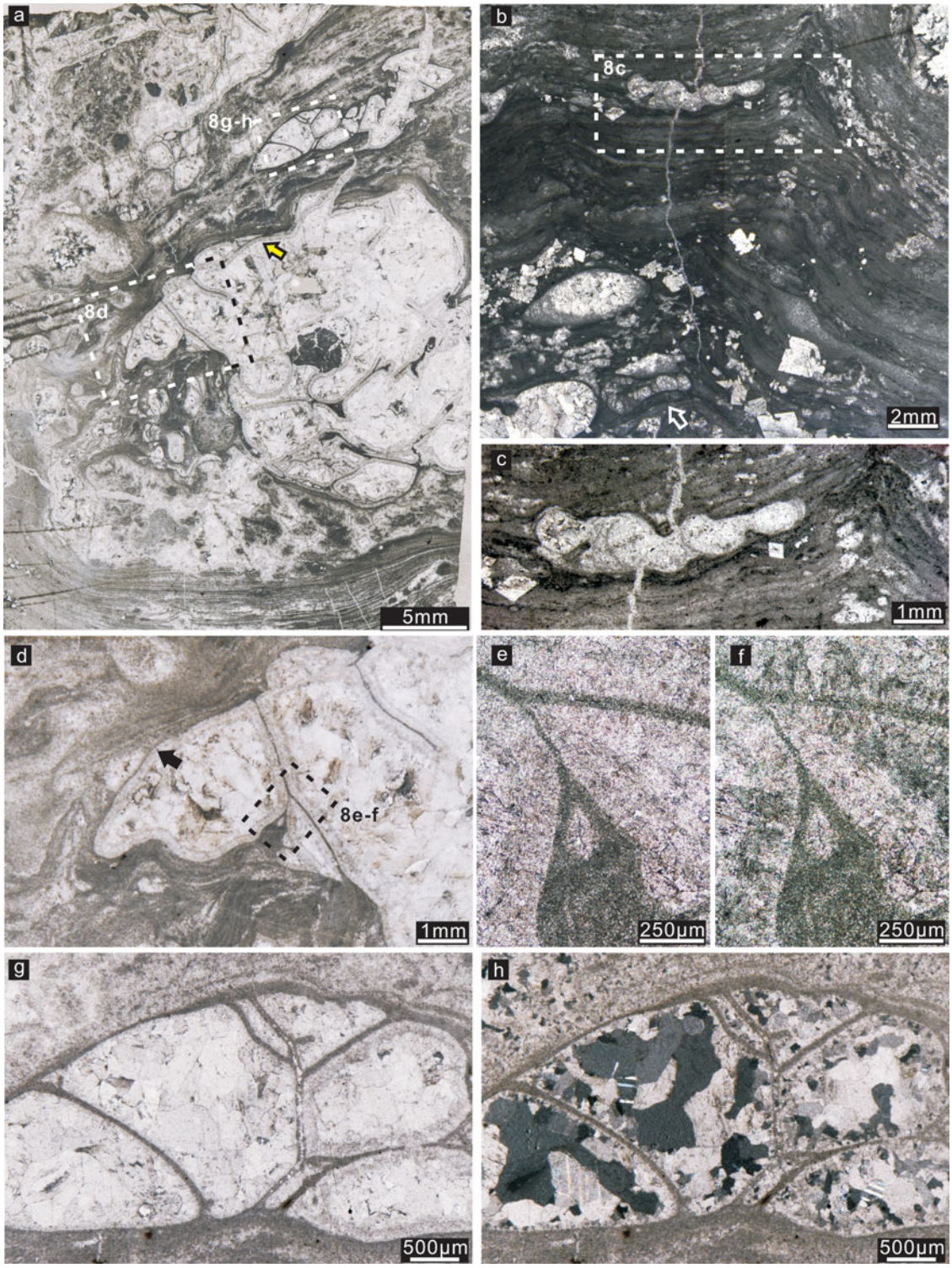

Figure 8. (Colour online) (a) Overview of a bulbous DYC-2 sample in thin-section. Areas in rectangles are enlarged in (d) and (g, h). The arrows in (a) and (d) indicate where a single lamina diverges from other laminae to form a thin wall. (b) Overview of lenticular DYC-2 in thin-section. The area in the dashed rectangle is enlarged in (c). The arrow indicates the chamber whose base conforms to the shape of the underlying laminae, while the upper part truncates the laminae at the same level. (c) Enlarged view of (b), illustrating the abruptly truncated laminae above the chambered structure. (d) An enlarged view of a part of (a), showing that contorted laminae merge to form thin walls. The area in the dashed rectangle is enlarged in (e, f). (e, f) Part of (d) observed in plane and crossed polarized light, respectively, showing that the walls are immediately overgrown by isopachous, bladed cements. (g, h) Part of (a) observed in plane and crossed polarized light, respectively. The chambers are surrounded by dark, continuous laminae, which are connected with the thin walls with direct contact and cuspate tubercles. The chamber walls are immediately overgrown by a thin layer of isopachous, bladed cements. The photos in (a) and (b) are oriented upwards. Sample numbers: (a), (d–h), Ls47; (b, c), Ls61.

https://doi.org/10.1017/S001675681700053X Published online by Cambridge University Press

Table 1. Comparison between Dengying and Cryogenian chambered structures

	Cryogenian chambered structures (Wallace *et al.* 2014)	Dengying chambered structures	
		DYC-1	DYC-2
Host rock	Clotted or indistinctly dendritic micritic masses	Microcrystalline dolomite with fenestral fabrics	Microcrystalline dolomite with microbially induced laminated fabrics
Chamber size	1–30 mm in diameter	Millimetric to centimetric	Millimetric to centimetric
Chamber cement	Isopachous, fibrous marine dolomite followed by late-stage coarsely crystalline dolomite or calcite	Isopachous, bladed cement followed by blocky spars	Isopachous, bladed cement followed by blocky spars
Chamber shape	Lobate, polygonal or dendritic; further divided into smaller chambers	Overall shape irregular; divided into polygonal subordinate chambers	Overall shape bulbous or lenticular; divided into polygonal subordinate chambers
Thick walls	Thick walls laminated, thin walls homogeneous; thickness 20–100 μm, up to 1 mm*	Laminated, up to hundreds of micrometres	Insignificant or indistinguishable from the host fabric
Thin walls		Homogeneous, 20–100 μm	Homogeneous, mainly 40–60 μm, up to hundreds of micrometres at irregularities
Mineralogy of walls	Micritic carbonate (now dolomite)	Microcrystalline dolomite	Microcrystalline dolomite
Growth form	Reefal framework; cavity fillings; intercolumnar among stromatolites	Encrusting; fenestrae-filling	Encrusting
Environment	Subtidal zone to deeper than 150 m	Evaporitic peritidal zone	Evaporitic peritidal zone

* The thicknesses of thick and thin walls were not described separately in Wallace *et al.* (2014).

Dengying structures is presented in Table 1, in which all the described characteristics of the former are summarized.

In spite of the similarity in basic construction, the Dengying structures still show variations from the Cryogenian analogues in a few aspects.

First, except for a few DYC-2 specimens, the overall shapes of the Ediacaran chambered structures cannot be assigned to the three morphological categories of Cryogenian chambered structures, namely, (1) lobate structures, which are encrusting bulbous chambers sometimes containing subdivided polygonal secondary chambers; (2) dendritic structures, which are elongated and branching chambers sporadically showing convex thin walls; and (3) polygonal structures, which are characterized by polygonal chambers, without any primary–secondary hierarchy or subdivision. The overall shapes of DYC-1 are either sheet-crack-like or irregular, while DYC-2 structures are either bulbous or lenticular. Nearly all the DYC-1 and -2 structures have subdivided chambers, i.e. their chamber walls are hierarchical.

Second, some lobate and dendritic forms of the Cryogenian structures are unequivocally frame builders (Wallace *et al.* 2014, 2015), while none of the Dengying structures appear to be frame building.

In addition, the Cryogenian structures from South Australia were estimated to have developed in a palaeo-water-depth of greater than 150 m (Wallace *et al.* 2015). The microbial member of the Rasthof Formation, where the Namibian chambered structures occur, exhibits subtidal facies (Le Ber *et al.* 2013). In comparison, the Dengying structures developed in a much shallower, peritidal environment.

4.b. Growth of the Dengying chambered structures

For both the Cryogenian and Dengying chambered structures, the features of the chamber walls are critical in deciphering their provenance. However, in the previous study of the Cryogenian chambered structures, this issue was not addressed in detail. Here, the close observation of the Dengying material allows a more comprehensive discussion.

The multi-laminated thick walls in DYC-1 samples may be disassembled into several individual laminae, which are similar to the homogeneous thin walls (e.g. Figs 5c, 7c–d). The DYC-2 samples lack prominent thick walls, but the host fabric *per se* is composed of thin microbial laminae. In both DYC-1 and -2, a thin wall can be formed by the innermost lamina of the surrounding multi-laminated system (i.e. the thick walls or the laminated host fabrics), which diverges from other laminae. In DYC-2, thin walls can additionally be formed by the convergence of multiple laminae. These phenomena indicate that the thick and thin walls, as well as the laminated fabric in DYC-2, have the same origin, and the continuous, uniform laminae are the basic building blocks of the chamber walls. In some cases, the thin walls appear to be strongly crinkled (Figs 7b), indicating that they possibly had a ductile stage before lithification. It is noteworthy that similar wall features have also been observed in some fragments of the Cryogenian chambered structures from Namibia (Fig. 7e, f).

https://doi.org/10.1017/S001675681700053X Published online by Cambridge University Press

In some DYC-1 samples (e.g. Ls45b), thick walls show a mode of inward accretion, where the innermost lamina overgrows the deformation of earlier laminae (Fig. 5c, g). This indicates that these DYC-1 structures occupied pre-existing fenestral cavities. Accordantly, these structures do not show any preferential growth orientation (Fig. 5a, b), and some gaps between the thick wall and cavity wall may have formed owing to the overgrowth of the former (e.g. Fig. 5b, d). However, for the other chambered structures, there are no definitive indicators for the accreting direction of the laminae in the thick wall.

In contrast to the fenestrae-filling DYC-1, the sheet-crack-like DYC-1 (sample Ls45a) shows a preferred upward growth orientation. This is reflected by the upper surface of these structures bearing many small, bulbous protrusions, which are nearly absent from their lower surface (Figs 3a, 4a, 6 and S2 in the online Supplementary Material available at http://journals.cambridge.org/geo). There is no trace of geopetal fillings that would be responsible for the flatness of the base. The small protrusions on the upper surface may represent new chambers in an initial stage, extending into the free space above the older parts.

Also, it seems that the bulbous DYC-2 chambers grew in a free space. In the consecutively ground sample Ls47, an interspace between two bulbous chambers is filled by sparitic cement. The smooth margin of the chambers and completeness of their overgrowing laminae indicate that this space was probably formed by growth, instead of erosion (Fig. 3e–g). Similarly, the lenticular DYC-2 chambers intercalated in laminated fabrics appear to have developed contemporaneously or paracontemporaneously with the microbial mat: the lower surface of the chambers generally conforms with the shape of the underlying laminae while the upper part of the chambers truncates the overlying laminae (Fig. 8b, c).

4.c. Interpretation of the chambered structures

Wallace *et al.* (2014) distinguished the Cryogenian chambered structures from fenestral cavities, travertine gas bubbles and methane release structures based on their well-defined, smooth and regular walls. The Dengying chambered structures can be differentiated from these inorganic structures for the same reasons. If not associated with microbial deposits, fenestral cavities and gas bubbles hardly have components comparable with the chamber walls. The laminated thick walls exhibit gaps at the contact with the cavity wall, and their innermost laminae can diverge to form thin walls, which subdivide the chamber space. These features distinguish them from inorganic precipitates lining cavity walls. Thin chamber walls are different from lithified bubble walls or precipitates between comparted substances by containing sub-circular holes. In addition, a few 'thin walls' in thin-section may represent filaments in 3-D space. For these reasons, here the discussion focuses on the possible biogenic provenances of the chambered structures, which have been addressed in the previous study: (1) proto-sponges, (2) calcimicrobes and microproblematica, and (3) microbialites.

4.c.1. Comparison with sponges

A few structures in Cryogenian carbonates have been suggested as body fossils of sponge-grade organisms, including *Otavia* from Namibia (Brain *et al.* 2012) and calcified irregular fragments from South Australia (Maloof *et al.* 2010). These materials are asymmetrical bodies containing cavities which are reminiscent of the aquiferous system of poriferans. However, other provenances, e.g. microbial deposits, protozoan fossils or depositional clasts, were not excluded for these structures (Antcliffe, Callow & Brasier, 2014). Chambered structures are apparently different from these structures in morphology.

The polymud fabric, which was mainly known from the Phanerozoic and related to degradative calcification of metazoan extracellular collagenous matrix, contains secondary voids associated with multiple generations of authigenic carbonate mud. This fabric has been reported from the Cryogenian Little Dal Group (Neuweiler, Turner & Burdige, 2009). However, the secondary voids in the polymud fabric are different from the chambers described here, in lacking smooth walls and often exhibiting geopetal fillings and scalloped margins.

Owing to their general shape, the Cryogenian lobate chambered structures were compared with the basal skeleton of some hypercalcified sponges, especially that of aporate sphinctozoans and labechiid stromatoporoids, although it was determined that the chambered structures are different from these sponge skeletons because of lacking pores and pillars (Wallace *et al.* 2014). A 'proto-sponge' affinity was proposed to interpret these disparities, and the lack of pores in the chamber walls was assumed to reflect osmotrophic feeding of primitive organisms. However, the organization and skeletalization of the hypothesized proto-sponges was not discussed.

The fossil skeletons of hypercalcified sponges were not confirmed as having poriferan affinity before the discovery of similar skeletons in modern Jamaican sponges (Hartman, 1969; Hartman & Goreau, 1970). Years of studies revealed that the known hypercalcified sponges secrete their basal skeletons either inside the soft tissue (e.g. *Vaceletia*) or outside the basopinacoderm (e.g. labechiid stromatoporoids), or intracellularly secrete calcitic spherulites and cement them exosomatically (e.g. *Astrosclera*) (Stearn, 1975, 2010; Wood, 1991; Reitner *et al.* 2001).

If the hypothesized proto-sponges adopted the first strategy, then chamber walls necessarily have pores, because pores serve not only as inhalant and exhalant openings, but also as paths through which the soft tissue is connected and could migrate (cf. Müller-Wille & Reitner, 1993; Vacelet, 2002). Although

https://doi.org/10.1017/S001675681700053X Published online by Cambridge University Press

sub-circular holes are observed in some chamber walls, it is difficult to confirm whether they represent organism growth or wall decay or mechanical destruction. If the proto-sponges secreted the skeletons outside the basopinacoderm while the soft tissue migrated, similar to labechiid stromatoporoids secreting their cysts, the derived skeletons would not have needed pores. However, cysts are single-layered and do not form multi-laminated structures (cf. Stearn *et al.* 1999). Finally, the chambered structures do not show any spherulite-like components corresponding to the third mode of skeleton construction.

In summary, the current understanding of sponge skeletogenesis does not support the scenario that a sponge-like organism could build skeletons like the chambered structures.

4.c.2 Comparison with calcimicrobes and microproblematica

Calcimicrobes and microproblematica are often composed of small elements, which are tens to hundreds of micrometres in size and show certain regular shapes, such as tubular, circular or botryoidal cells (e.g. Riding, 1991; Flügel, 2010). The investigated chambered structures are generally distinguishable from these fossils in exhibiting much larger (mostly millimetric to centimetric) and less regular subordinate chambers.

In spite of the size disparity, the lobate chambered structures may be reminiscent of the Palaeozoic microproblematicum *Wetheredella* Wood, 1948 in thin-section. However, *Wetheredella* is composed of non-septate, sub-circular tubes, while the Precambrian chambered structures do not have such a regular shape, and their lobate chambers can be further divided into polygonal subspaces.

The Mesozoic microproblematica *Lithocodium* and *Bacinella* resemble the chambered structures in containing spar-cemented cavities which are sometimes segmented by regular, thin micritic walls. However, these cavities are surrounded by thick, homogeneous micritic material and lack multi-laminated structures like the thick walls. In addition, the cavity system of many *Lithocodium* and *Bacinella* species is more elegantly organized than that of the chambered structures. For instance, in both type species *L. aggregatum* and *B. irregularis*, the cavity system consists of a prostrate and an erect part, and the latter is in the form of ramified filamentous tubes with reducing diameters (Schlagintweit, Bover-Arnal & Salas, 2010; Schlagintweit & Bover-Arnal, 2013). Because of their morphological complexity, these fossils were recently reinterpreted as algae or sponge bores (Schlagintweit, Bover-Arnal & Salas, 2010; Cherchi & Schroeder, 2012; Schlagintweit & Bover-Arnal, 2013).

In addition, the Cretaceous 'bacinellid textures' and 'lithocodoid-bacinelloid fabrics', which have been removed from *Bacinella* and *Lithocodium sensu stricto* and compared to calcified microbial mats, also exhibit chamber-like patterns confined by regular micritic walls in 2-D cross-sections (Neuweiler & Reitner, 1992; Schlagintweit, Bover-Arnal & Salas, 2010; Schlagintweit & Bover-Arnal, 2013). However, the 3-D architecture of these structures has not been studied. It is unknown whether their micritic walls are truly comparable with the thin walls of the Neoproterozoic chambered structures.

4.c.3. Comparison with microbialites

In fact, the laminae-based construction and growth pattern of the chambered structures readily indicate a microbialite interpretation. Especially in the DYC-2 samples shown in Figure 8, the thin walls are closely associated with microbial laminae in the surrounding fabrics. It is also conceivable that the biofilm-forming microbial consortia could have inhabited pre-existing fenestral cavities. They may have initially accreted on the cavity wall, then started to occupy the central space by developing angularly extending, single-laminated films (i.e. thin walls), and finally formed the fenestrae-filling DYC-1. The filamentous elements may represent the initiation of a thin wall, and the sub-circular holes in some thin walls possibly have resulted from biofilm decay. For chambered structures showing encrusting habits, the chamber space may have been produced by gas trapped in biofilms.

The real difficulty with the microbialite interpretation is finding an analogous laminae-based, chambered construction in known fossil or extent microbialites.

Many microbialites show chamber-like voids in thin-sections and polished slabs, but they are easily distinguishable from the Cryogenian and Dengying chambered structures because the void walls are irregular, without consistent thicknesses and smooth rims (e.g. Knoll, Wörndle & Kah, 2013; Wilmeth *et al.* 2015). The Archaean fenestrate microbialites consist of thin (1–10 μm), biofilm-like laminae that drape from thicker (100–300 μm) vertically oriented surfaces called 'supports'. Chamber-like voids are enclosed by the filmy laminae and supports (Sumner, 1997, 2000). The filmy laminae are similar to the thin walls of chambered structures in appearance (e.g. figs 2, 3 in Sumner, 2000). However, the Neoproterozoic chambered structures do not contain morphological elements corresponding to 'supports'. Furthermore, a recent study of some fenestrate microbialites of the plumose and plumose-cuspate forms revealed that their 3-D architectures are more complex than previously supposed. Tubular structures and interconnecting linear structures were newly identified (Rivera & Sumner, 2014). This further differentiates these Archaean microbialites from the chambered structures, because the latter are primarily constructed from smooth, continuous laminae, containing only a few filamentous elements and lacking tubular structures.

In modern photosynthetic microbial mats, accumulated oxygen produces cavities of different shapes, including bubbles, tubes and irregular blisters. Recent studies of cultured, cone-forming cyanobacteria

https://doi.org/10.1017/S001675681700053X Published online by Cambridge University Press

mats showed that surrounding these cavities, a dark, dense lamina associated with early precipitation of micritic high-Mg calcite can be formed (Bosak *et al.* 2009, 2010). This lamina is similar to the thin walls in the chambered structures, with consistent thicknesses varying from 20 μm to 150 μm (figs S4–S6 in Bosak *et al.* 2009; figs 5, 6 in Bosak *et al.* 2010). Moreover, this type of laminae appears to divide large voids, e.g. blisters, into irregular subordinate spaces (figs 2c, S5b in Bosak *et al.* 2009). However, apart from fossilization potential, these laminae only appear as single layers and were not reported as stacking to form multi-laminated structures like the thick walls in the Neoproterozoic chambered structures. In addition, the fenestrae-filling DYC-1 fossils are unlikely to be related to photosynthesis.

In summary, although some microbially induced structures, e.g. the 'bacinellid textures' and 'lithocodoid-bacinelloid fabrics' and the rapidly calcified laminae associated with photosynthesis-induced bubbles, share some common features with the Neoproterozoic chambered structures, there are still discrepancies. Further investigations and discoveries are required to ultimately decipher the biofilm-forming microbial consortia and associated environmental factors that produced the Neoproterozoic chambered structures.

5. Conclusions

The chambered structures from the Ediacaran Dengying Formation are comparable to the previously described Cryogenian chambered structures in basic construction. Their discovery in the Ediacaran indicates that chambered structures probably occurred more broadly in the fossil record than previously realized but were overlooked. As an example, the 'cellular crusts' from the Neoproterozoic Little Dal Group are also similar to the chambered structures according to the published description and illustration (Turner, Narbonne & James, 1993), but did not receive further investigation. Nonetheless, taking the 'cellular crusts' into account, the known records of chambered structures are still sparse and restricted to the Neoproterozoic.

The newly observed morphological details of the Dengying and some Cryogenian chambered structures indicate that the basic building blocks of the chamber walls are thin, homogeneous laminae, which primarily correspond to continuous surfaces in 3-D space. The morphology and growth pattern of these laminae distinguish the chambered structures from sponge skeletons and indicate a probable microbial origin. However, similar laminae-based, chambered constructions are yet unknown in fossil and extant microbialites.

New, relevant discoveries in the future are required to answer two overarching questions: (1) Do the chambered structures occur in other geological time periods? (2) What were the exact microbial consortia and/or environmental factors that produced these structures and made them construct reef frames in the Cryogenian?

Acknowledgements. We appreciate the suggestions from Prof. Junming Zhang (NIGPAS) for field trip preparation, and help from Dr Fangchen Zhao (NIGPAS) and Mr Zhaonian Wu (NIGPAS) with fieldwork. The comments from the two anonymous referees were valuable in improving the quality of the manuscript. This study was supported by the CAS Key Laboratory of Economic Stratigraphy and Palaeogeography, Nanjing Institute of Geology and Palaeontology and the Strategic Priority Research Program (B) of the Chinese Academy of Sciences (XDB18030304).

Supplementary material

To view supplementary material for this article, please visit https://doi.org/10.1017/S001675681700053X.

References

Ahn, S. Y. 2014. Basal Cambrian acritarchs biostratigraphy of the Yangtze Platform, South China. In *2014 GSA Annual Meeting, Vancouver, British Columbia, 19–22 October 2014*.

Antcliffe, J. B., Callow, R. H. T. & Brasier, M. D. 2014. Giving the early fossil record of sponges a squeeze. *Biological Reviews* **89**, 972–1004.

Bosak, T., Bush, J. W. M., Flynn, M. R., Liang, B., Ono, S., Petroff, A. P. & Sim, M. S. 2010. Formation and stability of oxygen-rich bubbles that shape photosynthetic mats: formation and stability of oxygen-rich bubbles. *Geobiology* **8**, 45–55.

Bosak, T., Liang, B., Sim, M. S. & Petroff, A. P. 2009. Morphological record of oxygenic photosynthesis in conical stromatolites. *Proceedings of the National Academy of Sciences* **106**, 10939–43.

Brain, C. K. 'Bob', Prave, A. R., Hoffmann, K.-H., Fallick, A. E., Botha, A., Herd, D. A., Sturrock, C., Young, I., Condon, D. J. & Allison, S. G. 2012. The first animals: ca. 760-million-year-old sponge-like fossils from Namibia. *South African Journal of Science* **108**, 658–65.

Cherchi, A. & Schroeder, R. 2012. Revision of the holotype of *Lithocodium aggregatum* Elliott, 1956 (Lower Cretaceous, Iraq): new interpretation as sponge–calcimicrobe consortium. *Facies* **59**, 49–57.

Condon, D., Zhu, M., Bowring, S., Wang, W., Yang, A. & Jin, Y. 2005. U–Pb ages from the Neoproterozoic Doushantuo Formation, China. *Science* **308** (5718), 95–8.

Erwin, D. H. 2015. Was the Ediacaran–Cambrian radiation a unique evolutionary event? *Paleobiology* **41**, 1–15.

Flügel, E. 2010. Cyanobacteria and calcimicrobes. In *Microfacies of Carbonate Rocks*, pp. 408–12. Berlin Heidelberg: Springer.

Giddings, J. A., Wallace, M. W. & Woon, E. M. S. 2009. Interglacial carbonates of the Cryogenian Umberatana Group, northern Flinders Ranges, South Australia. *Australian Journal of Earth Sciences* **56**, 907–25.

Grotzinger, J., Adams, E. W. & Schröder, S. 2005. Microbial–metazoan reefs of the terminal Proterozoic Nama Group (c. 550–543 Ma), Namibia. *Geological Magazine* **142**, 499–517.

Grotzinger, J. P., Watters, W. A. & Knoll, A. H. 2000. Calcified metazoans in thrombolite-stromatolite reefs of the terminal Proterozoic Nama Group, Namibia. *Paleobiology* **26**, 334–59.

Hartman, W. D. 1969. New genera and species of coralline sponges (Porifera) from Jamaica. *Postilla* **137**, 1–39.

Hartman, W. D. & Goreau, T. F. 1970. Jamaican corralline sponges: their morphology, ecology and fossil relatives. In *The Biology of the Porifera* (ed. W. G. Fry), pp. 205–43. Symposia of the Zoological Society of London 25. New York: American Press.

Knoll, A. H., Wörndle, S. & Kah, L. C. 2013. Covariance of microfossil assemblages and microbialite textures across an Upper Mesoproterozoic carbonate platform. *Palaios* **28**, 453–70.

Le Ber, E., Le Heron, D. P., Winterleitner, G., Bosence, D. W. J., Vining, B. A. & Kamona, F. 2013. Microbialite recovery in the aftermath of the Sturtian glaciation: insights from the Rasthof Formation, Namibia. *Sedimentary Geology* **294**, 1–12.

Lenton, T. M., Boyle, R. A., Poulton, S. W., Shields-Zhou, G. A. & Butterfield, N. J. 2014. Co-evolution of eukaryotes and ocean oxygenation in the Neoproterozoic era. *Nature Geoscience* **7**, 257–65.

Maloof, A. C., Rose, C. V., Beach, R., Samuelsson, B. M., Calmet, C. C., Erwin, D. H., Poirier, G. R., Yao, N. & Simons, F. J. 2010. Possible animal-body fossils in pre-Marinoan limestones from South Australia. *Nature Geoscience* **3**, 653–9.

Müller-Wille, S. & Reitner, J. 1993. Palaeobiological reconstruction of selected sphinctozoan sponges from the Cassian Beds (Lower Carnian) of the dolomites (Northern Italy). *Berliner Geowissenschafte Abhandlungen* (E) **9**, 253–81.

Neuweiler, F. & Reitner, J. 1992. Karbonatebänke mit *Lithocodium aggregatum* Elliott/*Bacinella irregularis* Radoicic. Paläobathymetrie, paläoökologie und stratigraphisches äquivalent zu thrombolithischen Mud Mounds. *Berliner Geowissenschafte Abhandlungen* **3**, 273–93.

Neuweiler, F., Turner, E. C. & Burdige, D. J. 2009. Early Neoproterozoic origin of the metazoan clade recorded in carbonate rock texture. *Geology* **37**, 475–8.

Penny, A. M., Wood, R., Curtis, A., Bowyer, F., Tostevin, R. & Hoffman, K.-H. 2014. Ediacaran metazoan reefs from the Nama Group, Namibia. *Science* **344** (6191), 1504–6.

Pratt, B. R. 1984. *Epiphyton* and *Renalcis*-diagenetic microfossils from calcification of coccoid blue-green algae. *American Association of Petroleum Geologists Bulletin* **54**, 948–71.

Reitner, J., Wörheide, G., Lange, R. & Schumann-Kindel, G. 2001. Coralline demosponges: a geobiological portrait. *Bulletin of the Tohoku University Museum* **1**, 219–35.

Riding, R. 1991. Calcified Cyanobacteria. In *Calcareous Algae and Stromatolites* (ed. R. Riding), pp. 55–87. Berlin, Heidelberg: Springer.

Riding, R. & Voronov, A. 1985. Morphological groups and series in Cambrian calcareous algae. In *Paleoalgology: Contemporary Research and Applications* (eds D. F. Toomey & M. H. Nitecki), pp. 56–78. Berlin, Heidelberg, New York, Tokyo: Springer-Verlag.

Rivera, M. J. & Sumner, D. Y. 2014. Unraveling the three-dimensional morphology of Archean microbialites. *Journal of Paleontology* **88**, 719–26.

Schlagintweit, F. & Bover-Arnal, T. 2013. Remarks on *Bačinella* Radoičić, 1959 (type species *B. irregularis*) and its representatives. *Facies* **59**, 59–73.

Schlagintweit, F., Bover-Arnal, T. & Salas, R. 2010. New insights into *Lithocodium aggregatum* Elliott 1956 and *Bacinella irregularis* Radoičić 1959 (Late Jurassic–Lower Cretaceous): two ulvophycean green algae (?Order Ulotrichales) with a heteromorphic life cycle (epilithic/euendolithic). *Facies* **56**, 509–47.

Stearn, C. W. 1975. The stromatoporoid animal. *Lethaia* **8**, 89–100.

Stearn, C. W. 2010. Part E, Revised, Volume 4, Chapter 9F: Functional morphology of the Paleozoic stromatoporoid skeleton. *Treatise Online* **8**, 1–26.

Stearn, C. W., Webby, B. D., Nestor, H. & Stock, C. W. 1999. Revised classification and terminology of Palaeozoic stromatoporoids. *Acta Palaeontologica Polonica* **44**, 1–70.

Sumner, D. Y. 1997. Late Archean calcite-microbe interactions: two morphologically distinct microbial communities that affected calcite nucleation differently. *Palaios* **12**, 302–18.

Sumner, D. Y. 2000. Microbial vs environmental influences on the morphology of Late Archean fenestrate microbialites. In *Microbial Sediments* (eds R. Riding & S. Awramik), pp. 307–14. Berlin, Heidelberg: Springer.

Turner, E. C., Narbonne, G. M. & James, N. P. 1993. Neoproterozoic reef microstructures from the Little Dal Group, northwestern Canada. *Geology* **21**, 259–62.

Vacelet, J. 2002. Recent 'Sphinctozoa', Order Verticillitida, Family Verticillitidae Steinmann, 1882. In *Systema Porifera* (eds J. N. A. Hooper, R. W. M. V. Soest & P. Willenz), pp. 1097–8. New York: Springer US.

Wallace, M. W., Hood, A. V. S., Woon, E. M. S., Giddings, J. A. & Fromhold, T. A. 2015. The Cryogenian Balcanoona reef complexes of the Northern Flinders Ranges: implications for Neoproterozoic ocean chemistry. *Palaeogeography, Palaeoclimatology, Palaeoecology* **417**, 320–36.

Wallace, M. W., Hood, A. V. S., Woon, E. M. S., Hoffmann, K.-H. & Reed, C. P. 2014. Enigmatic chambered structures in Cryogenian reefs: the oldest sponge-grade organisms? *Precambrian Research* **255**, 109–23.

Warren, J. K. 2006. Chapter 1: Interpreting evaporite texture. In *Evaporites: Sediments, Resources and Hydrocarbons*, pp. 1–57. Berlin, Heidelberg: Springer.

Wilmeth, D. T., Corsetti, F. A., Bisenic, N., Dornbos, S. Q., Oji, T. & Gonchigdorj, S. 2015. Punctuated growth of microbial cones within Early Cambrian oncoids, Bayan Gol Formation, Western Mongolia. *Palaios* **30**, 836–45.

Wood, A. 1948. '*Sphaerocodium*' a misinterpreted fossil from the Wenlock limestone. *Proceedings of the Geologists' Association* **59**, 9–22, IN2–IN5.

Wood, R. 1991. Non-spicular biomineralization in calcified demosponges. In *Fossil and Recent Sponges* (eds J. Reitner & H. Keupp), pp. 322–40. Berlin, Heidelberg: Springer-Verlag.

Wood, R. & Curtis, A. 2015. Extensive metazoan reefs from the Ediacaran Nama Group, Namibia: the rise of benthic suspension feeding. *Geobiology* **13**, 112–22.

Yang, B., Steiner, M., Zhu, M., Li, G., Liu, J. & Liu, P. 2016. Transitional Ediacaran–Cambrian small skeletal fossil assemblages from South China and Kazakhstan: implications for chronostratigraphy and metazoan evolution. *Precambrian Research* **285**, 202–15.

Yunnan Bureau of Geology and Mineral Resources. 1995. *Atlas of the Sedimentary Facies and Palaeogeography of Yunnan*. Kunming: Yunnan Science and Technology Press, 210 pp.

Zhu, T. & Luo, A. 1992. First discovery of an oldest *Renalcis* mound facies and its geological significance – an example from the upper Sinian Dengying Formation in northeastern Yunnan. *Sedimentary Geology and Tethyan Geology* **1992** (4), 20–8.

Zhu, M., Zhang, J. & Yang, A. 2007. Integrated Ediacaran (Sinian) chronostratigraphy of South China. *Palaeogeography, Palaeoclimatology, Palaeoecology* **254**, 7–61.

https://doi.org/10.1017/S001675681700053X Published online by Cambridge University Press